Electronics and Communications in Japan, Vol. 101, No. 4, 2018
Translated from Denki Gakkai Ronbunshi, Vol. 137-C, No. 10, October 2017, pp. 1329–1339

Regular Tetrahedral Lattice Coordinate System for an Equivalent Arrangement of Bio-mathematical Models Reflecting Objects' Shape

SATORU HONMA and HIDETOSHI WAKAMATSU
Graduate School of Health Care Sciences, Tokyo Medical and Dental University, Japan

SUMMARY

Mathematical simulation is utilized to visualize the invisible phenomena, such as distribution of temperature and/or stress in a concerning object, by using properly structuralized nodes on each grid point of the orthogonal coordinate system. Here, the close-packed nodes with same effective radius are set on the vertex of regular tetrahedrons. Thus, the mathematical simulation calculating the interactions among nodes can be appropriately performed on the newly proposed coordinate system, which consists of continuous connection of regular tetrahedrons with six basic lattices. Then, the regular tetrahedron lattice coordinate system is well confirmed for the description of definite nodes having interaction with their neighboring ones. © 2018 Wiley Periodicals, Inc. Electron Comm Jpn, 101(4): 42–54, 2018; Published online in Wiley Online Library (wileyonlinelibrary.com). DOI 10.1002/ecj.12048

Keywords: regular tetrahedral lattice coordinate system; node model; mathematical simulation; medical system; life innovation.

1. Introduction

Simulations using numerical models that mathematically represent causal relations between various phenomena based on results of scientific analysis [1, 2] can not only reproduce objects' dynamics but also predict possible abstract events from currently observed data, or estimate and visualize internal states imperceptible from outside, thus providing a plenty of useful information including uncertainties. In the field of medicine, effects of various therapy methods and intracorporeal biological activities are estimated without invasion into the body. Using these estimated biological activities in verification tests of medical equipment in terms of safety and effectiveness would make possible planning of clinical trials and studies as well as their shortening, thus contributing a great deal to the Life Innovation policy.

As regards mathematical models employed in simulations, compartment models [3] that focus on mathematical representation of input–output relations can be applied even in case when functions of body tissues are unexplained. With this approach, tissue internal states are set uniformly; therefore, when state distribution is assumed, node models with nodes placed at representative points of segmented tissues are more adequate [4–6]. In such models, simulation results are affected by node placement, and a number of purpose-specific placement methods were examined [7–11].

In finite element methods with nodes placed at arbitrarily selected test points, distance between nodes, connection number, and other parameters are not fixed, which is advantageous in that parameters can be set according to computer performance [4, 5].

On the other hand, if distance between nodes and connection number are fixed, then changes of parameters expressing physical characteristics become evident; thus, methods to place nodes at equispaced lattice points were also proposed [6–10]. As compared to compartment models and finite element methods, this may result in greater computational complexity or inaccurate shape representation. However, definite node positions are an advantage, while finer segmentation and more accurate calculation have become possible with the increase in computer performance.

By the way, when spheres of equal radius are closely packed so as to simplify calculations, their centers make up regular tetrahedrons. Maxwell showed that regular tetrahedron is a stable structure composed of the minimum number of lattice points [11]; hence a wide adoption of techniques in which regular tetrahedral structure is placed as a basic structure on orthogonal coordinates, being widely employed for spatial representation when developing calculation programs [6].

Lattice edges are arranged along cube face diagonals (below referred to as ''face diagonals'') so that tetrahedral

vertices coincide with lattice points in orthogonal coordinates; however, with continuous arrangement, two nonintersecting lattices run in parallel, and interaction does not necessarily occurs even between closely spaced nodes. A number of ways to solve this problem were proposed, such as connecting regular tetrahedrons with orthogonal coordinate grid, and tetrahedron arrangement combining face diagonals and cube interior diagonals (below referred to as ''space diagonals'') [6]. In so doing, however, distances between nodes and effective range shapes become complicated, thus obscuring physical properties of nodes, and adding to computational complexity. These issues are considered in detail in Appendix.

On the other hand, methods were proposed to reproduce human tissue shapes through continuous arrangement of regular tetrahedrons, independently of orthogonal coordinates [7, 8, 12]. In so doing, tetrahedron vertices are connected to those of other tetrahedrons, thus establishing pyramid-like connection relations; such relations are stored to a database, but search for correspondence relations may take time in case of a complex shape.

From this viewpoint, when placing nodes in a tetrahedral lattice, it would be appropriate to consider a coordinate system with continuous arrangement of tetrahedrons, and to present connection relations by certain rules that can be handled in the same way as in orthogonal coordinates. Nevertheless, there are no examples of connection relation rules for arbitrary shape arrangement in such tetrahedral coordinates. On the other hand, node allocation in lattice coordinates created by continuous arrangement of regular tetrahedrons was employed to propose dynamic models based on a visco-elasto-plastic model [1, 2, 9] and visualized models of temperature distribution in human head using a thermodynamic model [10]. Particularly, results of thermodynamic simulations using the latter model [13, 14] showed good agreement with results of experimental measurement, thus proving feasibility of accurate simulations with biomathematical models. However, regularity of node placement in such lattice coordinates was reported only fractionally [15], while calculation method was not described.

Considering the use of biomathematical simulations to contribute to the Life Innovation policy, in this paper we give a new definition of regular tetrahedral lattice coordinate system to express connection relations following certain rules. We clarify relations between nodes in this coordinate system, and establish a common algorithm of mathematical simulations with regard to interactions among nodes. Thus we clarify calculation procedures. In addition, we consider construction of object shapes in virtual space, and assess utility of this coordinate system through comparison with other coordinate systems.

2. Mathematical Model-Based Analysis

2.1 Use of node models

Conventional mathematical models are described via differential equations in space or time, and in many simulations, data observed at the current moment are used to calculate change or state at the next moment [1, 2]. In so doing, if results calculated one sampling before are taken as observed data, and spatial or temporal difference is set as small as possible, then nonlinear phenomena can be linearly approximated, and state transitions in time series can be continuously calculated. Due to linear approximation, time required for one computation shortens, but computational complexity grows as difference is set smaller. Thus, acceptable convergence error is defined with regard to arithmetic errors, and difference is set as small as possible in that range.

By the way, mathematical models include compartment models [3] that deal with real functional units when segmentation is difficult, and node models [4–10] that consider states in segmented areas so as to ensure following certain rules.

With compartment models focused on input–output relations, model parameters involve shape and size of areas in which internal states are assumed uniform. These models are especially useful when inputs and outputs can be fixed, being employed successfully in the field of medicine and pharmacology where input–output direction can be determined by blood flow.

On the other hand, node models, in which compartments are further segmented, prove appropriate when the model itself does not have any shape-dependent parameters, or when input–output direction cannot be determined uniquely. Nodal points represent mass, temperature, and other material characteristics around them. Normally, connection between nodes is expressed by *links*; however, in some cases such as spring models [1, 2, 9] and heat transfer models [10, 13, 14], connection elements should express energy transfer, attenuation, and accumulation as well. Thus in this study, we define *channels* to conceptually represent connections and respective energy transfer. In so doing, energy transfer, attenuation, and so on are only considered between nodes directly connected by channels. In other words, interactions occur only between two nodes directly connected by a channel, and these relations are represented by a mathematical model. Interactions between nodes not connected directly by channels are not taken into account; however, any arbitrary node is connected to multiple nodes depending on the node allocation, and eventually, interactions between all connected nodes are considered. Thus, a node model uses a combination of mathematical models representing actions of nodes and channels, respectively. When distance between nodes is small, mathematical models representing nodes and channels can be linearly

approximated by difference in calculation, and nonlinear properties can be expressed by functional units combining nodes and channels.

2.2 Common difference equations used in mathematical analysis

As explained above, in a node model, interactions between all nodes connected by channels are considered when state change of every node at the next moment is calculated from the current state using difference equations. State of particular node N_0 at moment t+1 one sampling ahead can be calculated from its state variable at moment t, a bias expressing state change caused by characteristics of that node itself, and interactions with n directly connected nodes N_i ($i = 1 \ \ldots \ n$). This can be described by the following general expression:

$$\xi_0(t+1) = \xi_0(t) + \sum_{i=1}^{n} \mathbf{k}_{i0}(t)\left\{\xi_i(t) - \xi_0(t)\right\} + \mathbf{B}_0(t). \tag{1}$$

Here ξ is vector variable expressing node's internal state, and $\mathbf{k}$ is coefficient matrix that changes state based on the difference of state variable. Besides, $\mathbf{B}$ is bias value. Subscripts attached to the vector variables denote number of nodes connected to the node N_0 for which state change is calculated; thus, ''$i0$'' indicates interaction that occurs between nodes N_0 and N_i.

Parameters expressing characteristics of each node and channel are set separately, and nodes' change states or energy transfer between nodal points is calculated using a unified method. When calculating changes in position, orientation, and shape of objects constructed with viscoelastoplastic models [2, 9], state variables are coordinate and velocity components of each node, while coefficient vectors express elasticity, viscosity, and plasticity. When calculating temperature distribution inside objects with heat transfer models [10], state variables are node temperatures, while coefficient vectors express heat transfer coefficients; here bias can be interpreted as amount of internally generated heat.

3. Building of Regular Tetrahedral Lattice Coordinate System

3.1 Base unit of node allocation

A node model represents states of each object's segment; therefore, nodes need to be allocated in space so as to reproduce object's shape. Assuming a uniform node's effective range and channel length, parameters of the mathematical model are directly related to object's properties. This offers an advantage of simpler discussion when considering simulation results. The range represented by a node can be defined as one within an effective radius around the node; that is, spherical ranges are obtained. If effective radius is set uniformly for all nodes, and the spheres contact each other to interact via channels, then the spheres are closely packed in space, and the nodes are arranged at the vertices of regular tetrahedrons. This is a part of arrangement known as close-packed hexagonal lattice (Fig. 1).

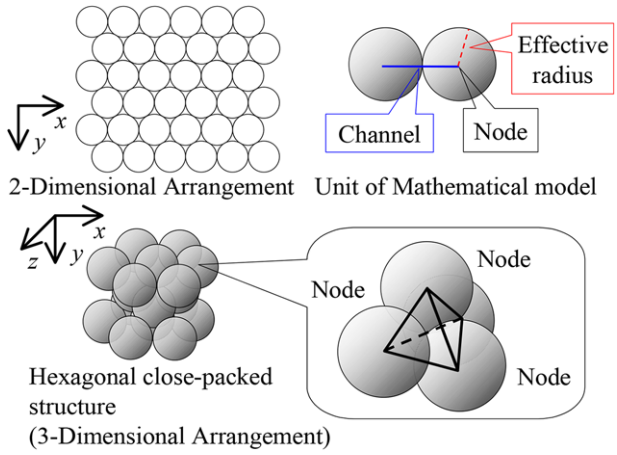

Fig. 1. Structural description of object with connections of nodes. [Color figure can be viewed at wileyonlinelibrary.com]

That is, when nodes are placed uniformly and closely in space, nodes exist at the vertices of a basic structure continuously configured of regular tetrahedrons.

3.2 Oblique coordinate system with continuously arranged tetrahedrons

In order to consider energy transfer between nodes or mass balance, connection relations between nodes must be clear. Let us define ''adjacency'' as a state when two particular nodes are connected directly by a channel and can interact with each other; then in a continuous tetrahedral arrangement, a node is adjacent to 12 other nodes as can be seen from Fig. 1. A coordinate system with continuously arranged regular tetrahedrons is established in order to manage numerous equispaced nodes and channels, and to determine, without overlap, up to 12 nodes interacting with a particular node. Every node and channel can be identified in such coordinate system by assigning a number based on the lattice coordinates.

When an arbitrary tetrahedron composed of adjacent nodes is selected, a regular triangular lattice made of continuously arranged regular triangles is obtained on a plane involving a face of the tetrahedron. This lattice represents

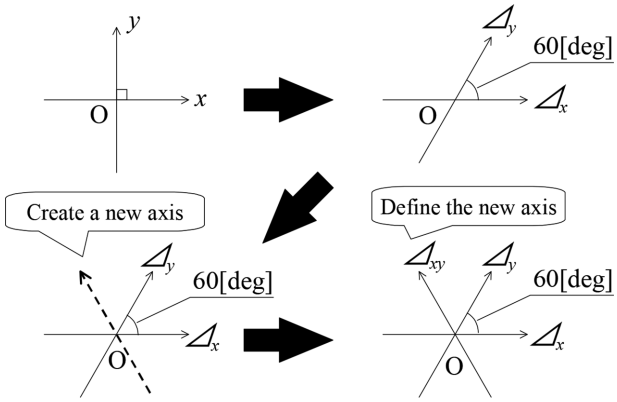

Fig. 2. Definition of basic axes in oblique coordinate system.

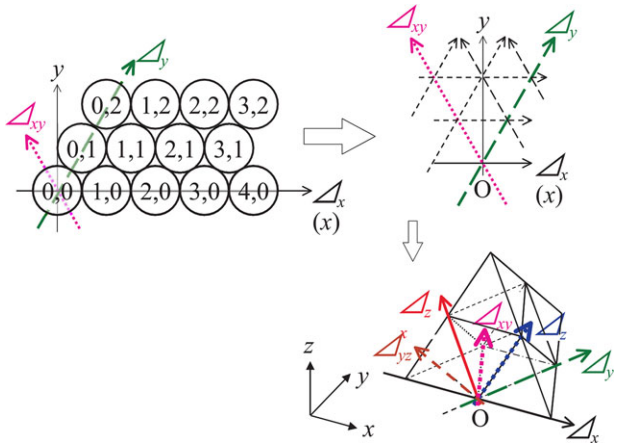

Fig. 3. Definition of six basic axes on oblique coordinate system. [Color figure can be viewed at wileyonlinelibrary.com]

oblique coordinates configured of extended sides of regular triangles and an infinite number of parallel lines. In case of three-dimensional (3D) arrangement, three pairs of opposite sides of a regular tetrahedron are skewed relative to each other; therefore, six coordinate axes are set up.

First, we set three basic axes, as in a conventional coordinate system. Specifically, a vertex of regular tetrahedron is defined as the origin, and three extended sides that connect the origin with other vertices are defined as Δ_x, Δ_y, and Δ_z. Any two out of these three axes intersect at an angle of 60° to make up respective planes. Another lattice intersecting with every axis at the origin at equal angles exists on plane $\Delta_x - \Delta_y$ made up of axes Δ_x and Δ_y. All nodes and channels are considered in mathematical simulations; therefore, channels existing on this lattice must be distinguished from those existing on parallel lattices. Thus we define Δ_{xy} axis as shown in Fig. 2. Besides, we also define axes Δ_{yz} and Δ_{zx} on planes $\Delta_y - \Delta_z$ and $\Delta_z - \Delta_x$. As a result, planes not containing the three axes Δ_x, Δ_y, and Δ_z on the faces of regular tetrahedron are obtained in parallel to the three axes Δ_{xy}, Δ_{yz}, and Δ_{zx}.

By the way, when a uniform calculation method is applied continuously, as is the case with mathematical simulations using node models, an efficient approach is to define array variables in a computer program, and to refer to the array variables by numbers assigned to every node. Oblique coordinates of any lattice point can be set up using the basic channel length and its integral multiples; therefore, oblique coordinates are expressed by indices of array variables, and characteristic values of respective nodes are recorded in these variables. The indices of array variables can be defined in 3D but such indices are normally specified using integers of 0 or greater, which is suitable for handling nodes existing in the first quadrant.

On the other hand, axes do not intersect in the oblique coordinates as explained above, and as compared to orthogonal coordinates, the area classified as the first quadrant amounts to 2/3 on a plane, and even less in 3D space, as shown in Fig. 3. Thus, when nodes are placed to reproduce an object's shape, the lattice coordinates must be translated so as to provide usable area corresponding to the object's size. In other words, with this method, one has to think about migration along the axes Δ_x, Δ_y, and Δ_z depending on the object's shape, which requires providing sufficiently large array domain, and therefore, sufficiently high computing power. From this standpoint, oblique coordinates assume restrictive conditions for node placement and mathematical simulations, which is not appropriate for general applications.

3.3 Definition of regular tetrahedral lattice coordinate system using basic lattice setting

If spheres of equal diameter are closely packed, and a straight line is drawn from the origin set at the center of an arbitrary sphere towards the center of an adjacent sphere, this line connects centers of contacting spheres. With this line defined as axis x of orthogonal coordinates, the other axis y can be selected in the direction passing through the center of a sphere in next nearest layer. Now consider a broken line that connects the two spheres through which axis y passes and the center of an adjacent sphere through which axis y does not pass, as shown in Fig. 4. A continuous broken line obtained by repeating this procedure is the closest to axis y in the oblique coordinates. If a lattice coordinate system different from the oblique coordinates is set up with reference to this broken line, then the lattice coordinates similar to orthogonal coordinates can be defined, and variable domain needed for calculation can be minimized.

In this study, a broken line obtained as explained above is defined as a basic lattice. The axes x and Δ_x are

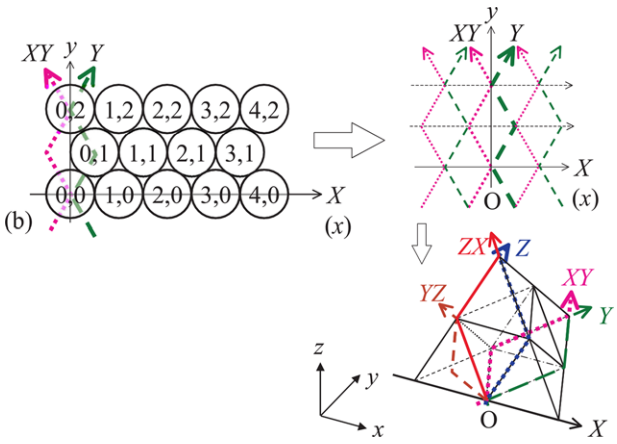

Fig. 4. Definition of six basic lattices on regular tetrahedral lattice coordinate system. [Color figure can be viewed at wileyonlinelibrary.com]

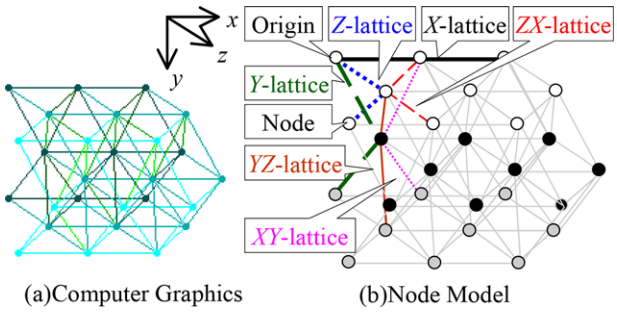

Fig. 5. Relationship between nodes and basic lattices in first quadrant (3D-Visualization): (a) representation of node array by CG, (b) correspondence between basic lattices. [Color figure can be viewed at wileyonlinelibrary.com]

straight lines but if they are exceptionally defined as basic *X*-lattice, then the said lattice closest to axis *y* orthogonal to basic *X*-lattice can be defined as basic *Y*-lattice. Further, a broken line symmetric to basic *Y*-lattice with respect to axis *y* can be defined as basic *XY*-lattice. Similarly, basic *Z*-lattice and basic *ZX*-lattice are defined with respect to basic *X*-lattice, and basic *YZ*-lattice is defined on the basic plane *YZ* made by basic *Y*-lattice and basic *Z*-lattice.

Figure 5 shows an object's shape with three nodes arranged in the direction of each basic lattice defined above. The diagram (a) pertains to 3D rendering by means of computer graphics, while diagram (b) explains relationship between the basic lattices *X*, *Y*, *Z* and *XY*, *YZ*, *ZX*. Here the lattices *XY*, *YZ*, and *ZX* are those parallel to basic *XY*-lattice, *YZ*-lattice, *ZX*-lattice and not passing the origin. Here colors of the basic lattices correspond to those in Fig. 4.

In Fig. 5, nodes are shown by circles; colors of the nodes are different depending on the lattice coordinates in the direction of basic *Y*-lattice. In other words, nodes

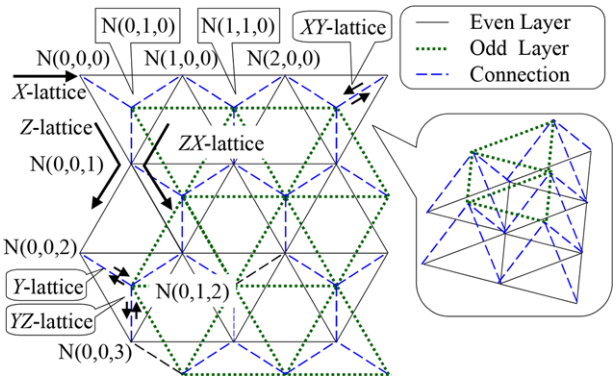

Fig. 6. Lattice coordinates and direction of basic lattices. [Color figure can be viewed at wileyonlinelibrary.com]

of same color lie on a plane *ZX* with same *Y*-lattice coordinates. As shown in the diagram, due to the definition of basic lattices, an area very close to that in orthogonal coordinates can be used as the first quadrant.

In this study, the coordinate system in which basic lattices and lattice coordinates are defined on coordinate system of continuously arranged regular tetrahedrons is called ''regular tetrahedral lattice coordinate system'' (below referred to as ''proposed coordinate system'').

3.4 Setting of lattice coordinates in regular tetrahedral lattice coordinate system

Lattice coordinates are defined to distinguish between lattice points made by the six basic lattices *X*, *Y*, *Z*, *XY*, *YZ*, *ZX* defined as explained above and lattices parallel to the basic lattices. In so doing, intersection of the basic *X*-, *Y*-, and *Z*-lattices set so as to coincide with the origin of the orthogonal coordinates is defined as the origin of the proposed coordinates. Any intersection between lattices is a lattice point; therefore, coordinates of every lattice point are specified with reference to the channel length, same as in the oblique coordinates. Therefore, the lattice coordinates are multiple of a basic length of respective basic lattice with respect to the origin, that is, integers of 0 or greater. In simulation of dynamic systems, node positions may shift; here we denote a node's initial position by N(*X*, *Y*, *Z*) using lattice coordinates (*X*, *Y*, *Z*). Besides, we denote variables in the proposed coordinates by uppercase symbols to distinguish them from variables in general orthogonal coordinates.

Relationship between overlap of planes parallel to *ZX*-plane as seen along axis *y* and basic lattices is illustrated in Fig. 6. The diagram shows lattice coordinates of some nodes and forward direction of lattices parallel to the basic lattices. When seen from this direction, layers with even *Y*-lattice coordinates (*Even layer*) and odd *Y*-lattice

coordinates (*Odd layer*) are stacked alternately with an offset. In such arrangement, *ZX*-plane coincides with the plane *zx* in orthogonal coordinates. At every *Y*-lattice coordinate, planes parallel to *ZX*-plane are connected by the basic *Y*-lattice, *XY*-lattice, and *YZ*-lattice (*Connection*). In so doing, *XY*-plane and *YZ*-plane, though not being conventional planes, are considered as reference planes in the proposed lattice coordinate system.

3.5 Channel identification using lattice coordinates

Channels that connect nodes lie on a lattice; thus, the channels can be identified using names of a basic lattice parallel to the lattice and lattice coordinates of one of the connected nodes on the lattice origin side. Thus, a name of the basic lattice is appended with hyphen to the channel symbol C_h, followed by the lattice coordinates of the start node. For example, $C_{h\text{-}X}(X, Y, Z)$ denotes a channel that connects nodes N(X, Y, Z) and (X+1, Y, Z) in parallel to the basic *X*-lattice.

The lattice coordinates are arranged along the basic *X*-, *Y*-, and Z-lattices so that only lattice coordinates X, Y, Z, respectively, are simply added for parallel lattices. On the other hand, assume that nodes connected on the basic *XY*-plane advance so that *Y*-lattice coordinate increments by 1. If the *Y*-lattice coordinate starts from an even node, then *X*-lattice coordinate decrements by 1; on the other hand, if the *Y*-lattice coordinate starts from an odd node, then *X*-lattice coordinate increments by 1, as can be seen from Figs. 4 and 6. Similarly, in case that nodes connected on the basic *ZX*-plane advance so that *Z*-lattice coordinate increments by 1, if the *Z*-lattice coordinate starts from an even node, then *X*-lattice coordinate decrements by 1; on the other hand, if the *Z*-lattice coordinate starts from an odd node, then *X*-lattice coordinate increments by 1. In case that nodes connected on the basic *YZ*-plane advance so that *Y*-lattice coordinate increments by 1, if the *Y*-lattice coordinate starts from an even node, then *Z*-lattice coordinate decrements by 1. In so doing, if the Z-lattice coordinate is even, then *X*-lattice coordinate decrements by 1; on the other hand, if the *Z*-lattice coordinate is odd, then *X*-lattice coordinate remains unchanged. If the *Y*-lattice coordinate starts from an odd node, then *Z*-lattice coordinate increments by 1. In so doing, if the *Z*-lattice coordinate starts from an even node, then *X*-lattice coordinate remains unchanged; on the other hand, if the *Z*-lattice coordinate starts from an odd node, then *X*-lattice coordinate increments by 1.

Thus, regarding a node N(X, Y, Z), the node's lattice coordinates depend on whether *Y*-lattice coordinates and Z-lattice coordinates are even or odd. This relationship is shown in Table 1. Here lattice coordinates of every channel are (X, Y, Z) because the channels connect Node 1 (start node) and Node 2 in parallel to the basic lattices.

Table 1. Relationship between the lattice coordinates of the nodes and the elements

	Layer		Code	
Kind of element	*Y*	*Z*	Node 1	Node 2
$C_{h\text{-}X}$			X, Y, Z	$X+1, Y, Z$
$C_{h\text{-}Y}$			X, Y, Z	$X, Y+1, Z$
$C_{h\text{-}Z}$			X, Y, Z	$X, Y, Z+1$
$C_{h\text{-}XY}$	even		X, Y, Z	$X-1, Y+1, Z$
	odd		X, Y, Z	$X+1, Y+1, Z$
$C_{h\text{-}ZX}$		even	X, Y, Z	$X-1, Y, Z+1$
		odd	X, Y, Z	$X+1, Y, Z+1$
$C_{h\text{-}YZ}$	even	even	X, Y, Z	$X-1, Y+1, Z-1$
	even	odd	X, Y, Z	$X, Y+1, Z-1$
	odd	even	X, Y, Z	$X, Y+1, Z+1$
	odd	odd	X, Y, Z	$X+1, Y+1, Z+1$

Irrespective of the values of *Y*- and *Z*-lattice coordinates, channels parallel to the basic *X*-, *Y*-, and *Z*-lattices are formed. On the other hand, with channels parallel to the basic *XY*-, *YZ*-, and *ZX*-planes, lattice coordinates of Node 2 change depending on *Y*- and *Z*-coordinates, thus making 11 combinations with parallel basic lattices, six of which are uniquely determined. In every lattice, channels exist before and after N(X, Y, Z); therefore, a total number of 12 channels connect to N, as explained above.

4. Arbitrary Shape Setting for Virtual Objects in Regular Tetrahedral Lattice System

4.1 Correspondence between lattice coordinates and orthogonal coordinates

In many cases, real coordinates defined in orthogonal coordinate system or oblique coordinate system do not coincide with lattice coordinates. Thus we explain about conversion equations that establish correspondence between lattice coordinates and orthogonal coordinates.

In the proposed coordinates, lattice points are placed by the rules described above; therefore, real coordinates (x_{real}, y_{real}, and z_{real}) in orthogonal coordinate system can be expressed using lattice coordinates (X, Y, Z) and lattice basic length l as shown below. In so doing, the origin of the proposed coordinates coincides with that of orthogonal coordinates. As regards 'mod' in the following expressions, 'A mod B' denotes the remainder of dividing A by B.

Thus, positions of lattice points in the lattice coordinate system can be uniquely determined, and nodes can be arranged according to an arbitrary object's shape.

$$x_{\mathrm{real}} = \left[X + \{(Y+1) \bmod 2 + (Z+1) \bmod 2\}/2\right] \times l, \tag{2}$$

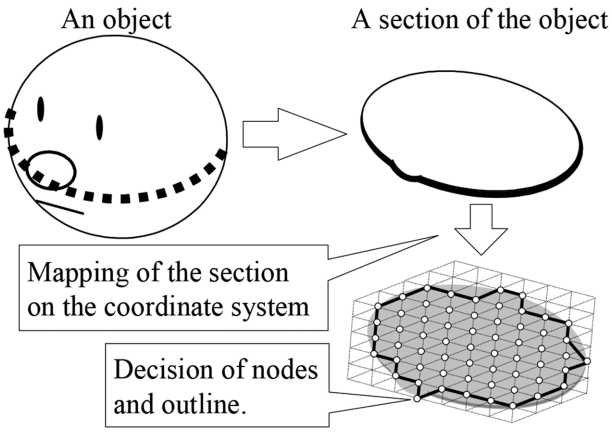

Fig. 7. Arrangement of nodes according to shape of objects' cross-section.

$$y_{\text{real}} = Y \times \sqrt{6}/3 \times l, \tag{3}$$

$$z_{\text{real}} = \left[Z \times \sqrt{3}/2 + \{(Y+1) \bmod 2\} \times \sqrt{3}/6 \right] \times l. \tag{4}$$

4.2 Reproduction of object's shape in regular tetrahedral lattice coordinate system

Influence of object's shape cannot be ignored in mathematical simulations when objects affect each other and environment, for example, when objects collide during motion, or exchange heat with environment. With node-based simulation methods, nodes can be placed arbitrarily with regard to basic channel length, which makes it possible to reproduce object's shapes.

In the lattice coordinate system defined above, there is a horizontal offset between *ZX*-plane and parallel planes depending on the *Y*-lattice coordinate; however, unevenness within the planes is small, and they can be handled as a horizontal plane in orthogonal coordinates. As regards objects of mathematical simulations, we assume a cross-section in horizontal direction as shown in Fig. 7, and map this shape onto the lattice coordinates. The nodes within the mapped area make up the object of simulation. If nodes are allocated at uniform intervals in each selected cross-section of an object, then the object's shape can be reproduced in the lattice coordinates.

By the way, in the lattice coordinates, discretization is performed using basic channel length and thus determined height of regular tetrahedrons so that object's shape cannot be perfectly reproduced. However, with channel length set sufficiently short, reproduction of fine shapes becomes possible, and the said discretization does not impair mathematical simulations.

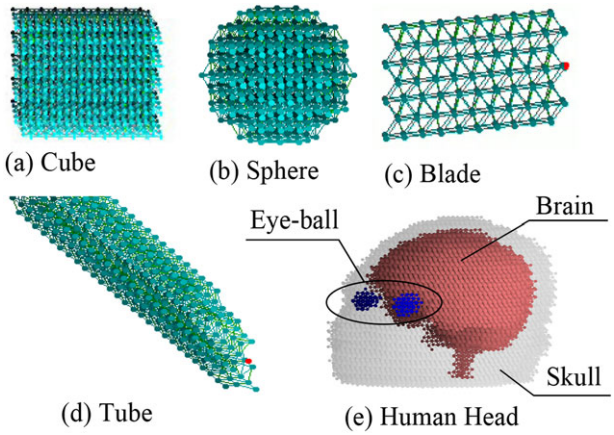

Fig. 8. Various shapes of objects constructed as set of nodes. [Color figure can be viewed at wileyonlinelibrary.com]

4.3 Various shapes constructed in regular tetrahedral lattice coordinate system

Examples of arbitrary node allocation in the proposed coordinate system are given in Fig. 8 [1, 2, 9, 10]. Particularly, the diagram (a) [1, 2, 9] pertains to a rectangular parallelepiped with the same number of nodes placed along basic *X*-, *Y*-, and *Z*-axes. In the diagram (b) [1, 2, 9], a spherical region is specified by nodes allocated around an arbitrary node. The diagram (c) [2] is a plate-like object with the thickness along basic *Z*-lattice configured by two layers. The diagram (d) [1, 2, 9] pertains to a tubular object represented by a double cylinder around the basic X-lattice, nodes being continuously connected on the inner side of external cylinder and outer side of internal cylinder. The diagram (e) [9, 10] represents a skull shape with brain, eyeball, muscle, skin, and other elements of the human head. This model represents by applying the proposed method to an MRI scans acquired at equal intervals. With conventional MRI, slice intervals are set to 1 to 10 mm; in the diagram (e), nodes are spaced at 6 mm. Figure 9 shows an example of node placement in the brain area of a sagittal plane scan obtained by MRI, and used to build the model in Fig. 8(e); this node placement offers good agreement with the MRI scan.

By the way, though most of biological objects have a definite shape, small deformations of several millimeters constantly occur; thus, one can think that the shapes can be properly reproduced if node's effective radius is 10 mm or less. In addition, even if node spacing is set to 1 mm for higher resolution and accurate shape reproduction, this

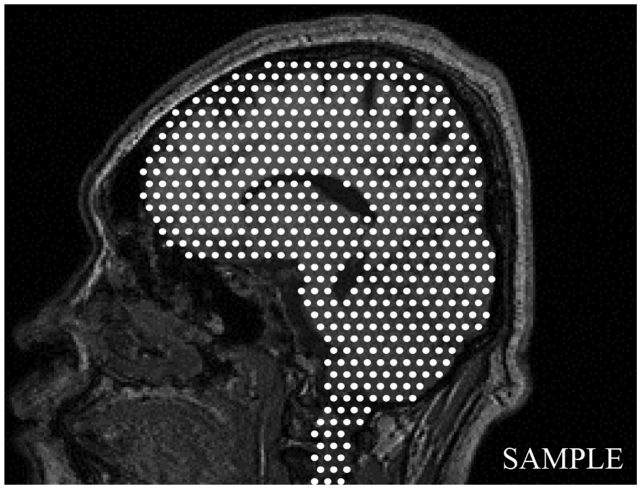

Fig. 9. Example of node placement based on MRI image.

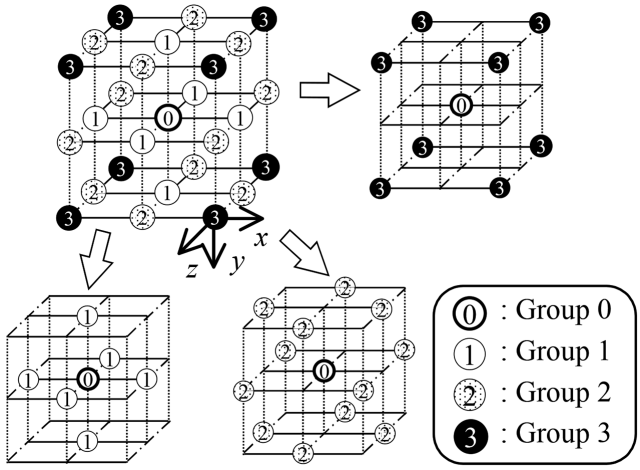

Fig. 10. Relation among nodes in orthogonal coordinate system.

can be supported in the proposed coordinate system by expanding coordinate domain.

Thus, arbitrary shapes can be sufficiently reproduced with a node set using the proposed method.

5. Comparison with Node Allocation Methods Using Orthogonal Coordinates

5.1 Nonequivalence of nodes in orthogonal coordinates

With conventionally used orthogonal coordinates, any two out of the three basic axes *x*, *y*, *z* are perpendicular to each other; thus, space is divided equiangularly using as few basic axes as possible. In so doing, the number of dimensions is the same as the number of basic axes that ensures intuitive coordinate assignment.

When lattice coordinates are set in orthogonal coordinate system as is often the case with mathematical simulations, interactions are calculated between a node ⓪ and vertices of eight cubes that have a common vertex at that node, as shown in Fig. 10. Lattices can be constructed using the three coordinate axes *x*, *y*, *z* and their parallel axes; in doing so, nodes that may interact with node ⓪ are divided into three groups depending on distance–-Group ① connected by cube sides, Group ② connected by face diagonals, and Group ③ connected by space diagonals. The Groups ①, ②, and ③ contain 6, 12, and 8 nodes, respectively.

In this study, we assumed that all nodes are uniform as explained in Section 2.1, and that interactions occur when nodes' effective ranges come into contact. Therefore, in orthogonal coordinates, nodes of Groups ② and ③ are not in contact at a distance where nodes of Group ① are; that is, based on the rule described in Eq. (1), these groups do not interact. Thus, calculations are conducted with regard to Group ① only, which results in less computation as compared to the proposed coordinate system. In so doing, influence of Groups ② and ③ propagates to respective contacting nodes with a delay of one or two time-steps.

However, when a tetrahedral structure is configured of regular tetrahedrons and rectangular triangular pyramids [6], interactions with nodes of Group ② are also taken into account with regard to distance. In this case, influence of Group ② has two stages–-direct influence at moment t and indirect influence via Group ① at moment t+1. As a result, the difference equation in Eq. (1) and prerequisites are different; thus, computational complexity increases when all lattice lengths are same in the proposed coordinate system and nodes are placed with same density. Besides, one has to consider possible arithmetic errors due to time delays. Influence of nodes of Group ③ was also mentioned [6], but in doing so, the prerequisite of constructing cubes from tetrahedrons is ignored. Moreover, influence of Group ③ is set in three stages including indirect influence via Groups ② and ① at moments t+1 and t+2; as a result, the influence of time delays grows as compared to the case when only Group ② is taken into account.

In addition, tetrahedral structures are stable structures according to Maxwell's equation [11], while cubic structures have been proven to be unstable structures. Therefore, considering shape variation in dynamic models, shape can be maintained in tetrahedral structure with appropriate parameter setting, but cannot be maintained in cubic structure. Besides, in tetrahedral structure, shape is maintained using minimum truss configuration, which means nonexistence of multiple interaction channels and ensures regular arithmetics.

From these viewpoints, lattice coordinates set in orthogonal coordinate system are advantageous in that correspondence among nodes is easily intuitive. On the other hand, efficiency of mathematical simulations may be impaired in some cases because it is difficult to achieve shape maintenance and unification of calculation.

5.2 Comparison of space utilization in terms of node fill factor

Spherical nodes adjoin at a point of contact, and form spaces enclosed by spheres. These spaces are not included in any node so that calculations become impossible inside them.

The proposed coordinate system is a close-packed hexagonal lattice, and therefore, the node fill factor is about 74% [16]. On the other hand, the node fill factor is about 52% when nodes are placed at lattice points in orthogonal coordinate system as shown in Fig. 9, and nodes do not exist inside the lattice or on the lattice plane. That is, in the proposed coordinate system, incomputable domain decreases by about 55%.

If node radius is sufficiently small, then hardly any difference occurs between adjacent nodes; considering that shape errors occur in biological objects as mentioned above, states inside the incomputable regions can be approximated by state of any neighbor nodes within the margin of arithmetic error.

Thus, when the proposed coordinate system is used in biomathematical simulations, the most of analytic space is computable.

5.3 Accuracy evaluation of mathematical operations in each coordinate system

In order to estimate accuracy of calculated results depending on the coordinate system, we consider visualization of temperature distribution in the brain [10, 14], and compare mathematical simulation with experiments on human head models assuming that brain temperature is controlled by selective hypothermic treatment. That is, in the mathematical calculation, Fourier's law of heat conduction [16] is applied to the mathematical model of human head shown in Fig. 11 to calculate temperature distribution in the brain, and brain temperature control assuming external input is performed. Specifically, 40^3 (= 64,000) nodes are arranged along each of axes X, Y, Z, and the model is divided into six organs-– *Brain*, *Skin*, *Skull*, *Eyeball*, *Blood vessel*, and *Cerebrospinal fluid*. Nodes not belonging to any of these are expressed as *Air*. Heat capacity, heat transfer coefficient, initial temperature, and metabolic heat production of each organ and air are taken from the literature [10]. At the moment

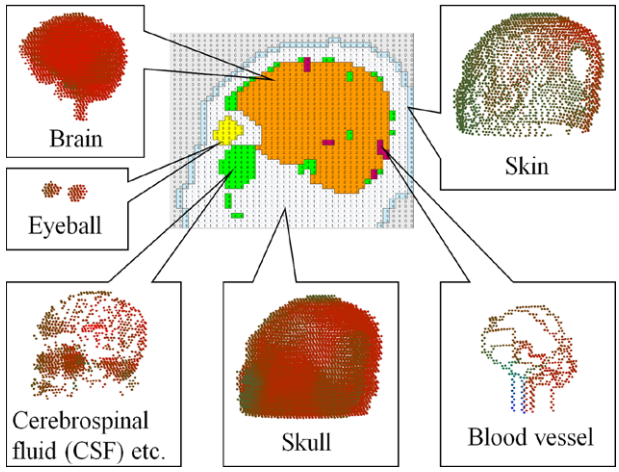

Fig. 11. Classification of brain tissue model. [Color figure can be viewed at wileyonlinelibrary.com]

when brain metabolism doubles from its initial value and brain temperature reaches 39 °C, brain temperature control using selective hypothermic treatment is applied with the target temperature of 35 °C. As regards selective hypothermic treatment, we applied a cooling model in which simple cooling is switched over to temperature management based on a control theory as proposed by Honma and colleagues [14]; the control theory was based on control laws combining adaptive gain control and integral control [17]. In doing so, Ringer's solution at certain temperature is injected into a part of feeding vessels toward the brain, and temperature-adjusted blood obtained through mixing with blood of normal temperature injected from the other vessels circulates in the brain so that heat is exchanged inside the brain. In both simulation and model experiments, temperature-adjusted Ringer's solution is injected in the right and left internal carotid artery, while normal blood at 37 °C is injected in the right and left vertebral artery. Temperature of Ringer's solution is adjusted in a tank through mixing cold and hot water. Flow rate of cold and hot water pumps is set to catalog values of the model experiment system. The tanks of cold and hot water are provided with a cooler and a heater, respectively, to maintain set temperatures during circulation. Performance of the cooler and the heater is set to catalog values of the model experiment system. In case that supply of cold and hot water becomes short in course of experiment, Ringer's solution temperature is set within a feasible range. Besides, in simulation, a compartment model ignoring temperature distributions in cold and hot water tanks is employed; time interval of one cycle is set to 1 s.

The simulation program is written in Microsoft Visual C++ 2010 Express, and run on an ordinary PC (Windows 7, CPU: Core i5-3320M (2.60 GHz), 3.20 GB memory).

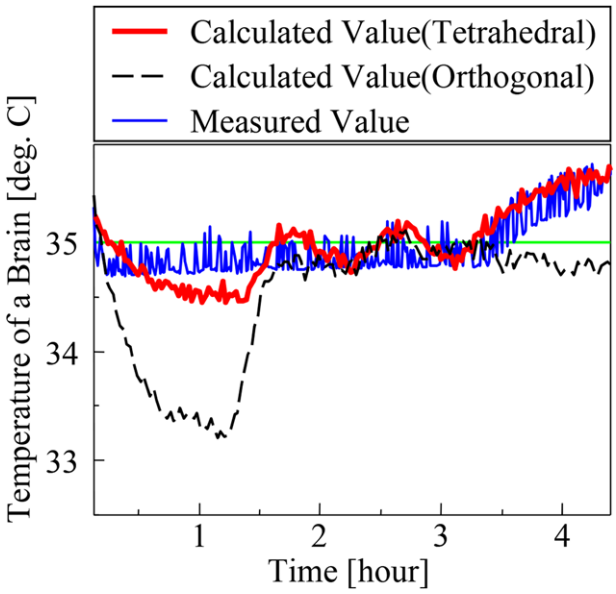

Fig. 12. Comparison of two mathematical simulations with different coordinate systems and model experiment measurements. [Color figure can be viewed at wileyonlinelibrary.com]

The mathematical model is calculated using both the proposed coordinates and orthogonal coordinates. Aiming at higher calculation accuracy, the mentioned Group ③ is also taken into account in the case of orthogonal coordinate system. Only heat transfer coefficient [10] that depends on distance between nodes is appropriately adjusted, while all other calculation conditions are unchanged. In the simulation, air temperature is approximated by a sine wave of 25 ± 1 °C with a period of 1.5 h based on the experimental values. The human head model is fabricated with the shape same as the mathematical model, and the same algorithm is used in the experiments for temperature control. In both mathematical simulation and model experiments, a dead band of 0.2 °C is set considering effects of observation noise.

5.4 Comparison of calculation results and mockup experiment results for each coordinate system

The calculated and measured results are presented in Fig. 12. In both simulation and experiments, temperature control starts from the moment when the brain temperature is at its target +0.3 °C, which corresponds to 0 on the time scale. The time worth of 20,000s computation in the simulations was about 384 s for the proposed coordinates and about 495 s for orthogonal coordinates.

In the model experiments, temperature of cold water rose in 3 h after the beginning, and temperature management became impossible so that the brain is heated up, which was reproduced in the simulation using the proposed coordinate system. On the other hand, these simulated results are lower by 0.2 °C at maximum as compared to the model experiments at 0 to 1.5 h. This means that overshoot produced by the past simple cooling is bigger than in the experiments. The cooler has same performance in the simulations and experiments, but the experimental cold water tank exchanges heat with the atmosphere so that the temperature slightly exceeds its set value (5 °C). On the other hand, a compartment model is sued in the simulations to reproduce dynamics of the cold water tank; in doing so, the heat exchange with the atmosphere is not regarded, while the cooler efficiency is assumed to be 100%, so that the temperature decreases just to its set value. During simple cooling in the temperature management, temperature of Ringer's solution is almost same as that of cold water, which can explain that cooling effect in the simulations is higher than in the model experiments. However, discrepancy with the measured values is basically within ±0.5 °C, which can be recognized as a good reproduction of the experimental results. In contrast, in case of the orthogonal coordinates, the error grows as big as 2°; moreover, the mentioned rise of brain temperature is not reflected. That is, the orthogonal coordinate system reproduces the experiments to some extent, but this reproduction can be hardly called adequate. Our results indicate that as compared to orthogonal coordinates, the proposed coordinate system ensures more realistic and accurate mathematical simulations.

5.5 Utility of simulations using regular tetrahedral coordinate system

In the proposed coordinate system, regular tetrahedrons with stable structure are continuously allocated, and basic lattices are formed by certain rules to achieve place utilization of the same order as in orthogonal coordinates. In doing so, real coordinates of all nodes placed at lattice points are determined using lattice coordinates so that arbitrary shapes can be easily constructed. The nodes at lattice points are closely packed and basically equivalent to orthogonal coordinates; channels that connect nodes lie on respective lattices.

A node has 12 adjacent nodes, and as compared to orthogonal coordinates, energy transfer is treated regularly using a unified procedure. Also, node fill factor is higher than in orthogonal coordinates; as a result, incomputable domain is reduced, and computation accuracy remains or improves. On the other hand, the basic *Y*- and *Z*-lattices are broken lines that change their direction at every lattice point; therefore, channels placed on the basic *XY*-, *YZ*, and *ZY*-lattices and parallel lattices not coincident with orthogonal coordinate axes cannot be sequentially identified through simple coordinate increment, as distinct from

a coordinate system with axes defined as straight lines. However, certain regularity is confirmed from *Y*- and *Z*-lattice coordinates of start points, which can be incorporated into a calculation program. Thus, simulations using this coordinate system can be easily implemented.

However, when reproducing nonbiological fixed shapes, some errors may occur in the proposed method as compared to free mesh techniques where nodes are allocated according to object's shape without setting lattice points in space [4, 5]. However, biological objects assumed in the proposed method may change their shape by several centimeters over time; therefore, one can expect sufficient reproduction of object's shape if distance between nodes is set as necessary so that shape changes can be considered within error range.

Comparison between the model experiments and mathematical simulations suggests that the proposed coordinate system agrees with measured values better than orthogonal coordinate system. The number of channels calculated at each node is 26 in orthogonal coordinates and 12 in the proposed coordinates, which results in lower computational complexity and faster simulations. Calculation time includes components common for each coordinate system such as drawing time so that the total time does not halves, but we showed that the computational complexity is reduced more than two times, while calculation accuracy is high. As mentioned above, in orthogonal coordinates, response of temperature control slows down because of time delays caused by three-stage propagation, which may explain the bigger cooling effect observed from 0 through 1.5 h, and the deviation observed after 1.5 h. One can also think of errors caused by the difference in node fill factor.

Apart from the results presented in Fig. 12, studies using mathematical models with continuous arrangement of regular tetrahedrons [1, 13, 14], same as in the present study, showed relatively good agreement between simulated and measured results for different algorithms of temperature control. Together with the results of this study, it confirms that the proposed method is sufficiently useful in practice.

6. Conclusion

In this study, we proposed a regular tetrahedral lattice coordinate system applicable to biomathematical simulations using node models. This coordinate system combines advantages of orthogonal coordinates (easy shape setting) and oblique coordinates (stable structure), thus being suitable for mathematical simulations that reproduce object's shapes. In addition, the number of adjacent node is reduced to required minimum; as a result, computing time to calculate interactions is reduced, while close-packed and uniform node placement is advantageous for real-time visualization of continuous distributions of state changes. Furthermore, as compared to tetrahedrons placed on cubic lattice, interactions are treated regularly, thus preventing logical contradictions.

In the proposed method, nodes are arranged uniformly so that shape reproduction is not perfect; however, considering temporal change of biological shapes, various mathematical models can be supported as long as distance between nodes is set sufficiently small. Besides, continuous state distributions can be visualized because most of space is defined as computable domain. The proposed method was verified for dynamic models [1, 2, 9] and thermodynamic models [10, 13, 14]; the method combines a number of features advantageous for a wide variety of biomathematical simulations. Moreover, this study may develop into an efficient versatile method in a wide range including calculation of density distributions due to mass transfer. That is, the method is also useful as a basis for standard evaluation procedures to confirm safety and effectivity of revolutionary medical technologies in the framework of Life Innovation.

Acknowledgment

This study was in part subsidized by JSPS Grant-in-Aid for Scientific Research (JP17K01405).

REFERENCES

1. Wakamatsu H, Honma S. Visual representation and its applications to virtual reality. Kyoritsu Shuppan, Tokyo; 2011. (in Japanese)
2. Honma S, Wakamatsu H. Distortion and destruction of virtual objects using various kinds of haptic systems. J Soc Instru Contr Eng 2012;51(10):968–982. (in Japanese)
3. Liang Z, Chenguang D. Theoretical simulation of temperature distribution in the brain during mild hypothermia treatment for brain injury. Med Biol Eng Comput 2001;39:681–687.
4. Brian HD, Robert CE, George SD et al. Finite element simulation of cooling of realistic 3-D human head and neck. J Biomech Eng 2003;125(6):832–840.
5. Yassene M, Janko FV. A finite element method model to simulate laser interstitial thermo therapy in anatomical inhomogeneous regions. Biomed Eng Online 2005;4(2).
6. Hansmartin F, Sophia H, Aldo S et al. Tetrahedral mesh generation based on space indicator functions. Int J Numer Methods Eng 2013;93(10):1040–1056.
7. Isabelle B, Jeremie P, Line G. A new characterization of simple elements in a tetrahedral mesh. Graph Models 2005;67:260–284.
8. Manuel S. Real-time isosurface extraction with view-dependent level of detail and applications. Comput Graph Forum 2015;34(1):103–115.

9. Wakamatsu H, Honma S. Construction and manipulation of virtual continuum object using visco-elasto-plastic tetrahedron elements for haptic system. Int J Math Models Methods Appl Sci 2011;5(4):738–746.
10. Honma S, Takagi Y, Wakamatsu H. 3D-visualized model of temperature distribution in the brain for the investigation of brain cooling effect. Electron Commun Jpn 2014;97(11):56–64.
11. Hangai Y, Kawagichi K. Shape analysis: Generalized matrices and their applications. Baifukan, Tokyo; 1991. (in Japanese)
12. Kup-Sze C, Hanqiu S, Pheng-Aim H. An efficient and scalable deformable model for virtual reality-based medical applications. Artif Intell Med 2004;32:51–69.
13. Takagi Y, Honma S, Wakamatsu H et al. Comparison of brain temperature distribution between mathematical and solid models of head thermal characteristics. Elec Eng Jpn 2015;193(2):58–68.
14. Honma S, Wakamatsu H. Control methods for the precise brain temperature management in selective brain hypothermia therapy. IEEJ Trans EIS 2016;36(4):525–531. (in Japanese)
15. Honma S, Wakamatsu H. Proposal of regular tetrahedron lattice coordinate system for a mathematical description of various simulations. The Special Interest Group Technical Reports of IPSJ, 2014-CG-156, No 3, IPSJ-CG14156003, 2014. (in Japanese)
16. Ooki M, Oosawa T, Tanaka M et al. (ed.): Encyclopedical dictionary of chemistry. Tokyo Kagaku Dojin, Tokyo; 1989. (in Japanese)
17. Honma S, Wakamatsu H. Control of selective brain hypothermia by adaptive gain and integral action. Annual Meeting Record IEE Japan, vol 3, No 3-002, p 2–3 2017. (in Japanese)

APPENDIX

A number of methods were proposed to arrange tetrahedrons in orthogonal coordinate system. Here we give a graphic overview of previously proposed methods as well as our comments.

A regular tetrahedron configured by connection of diagonals on cube faces shares four cube vertices as shown in Fig. A1. By continuous arrangement of such tetrahedrons, a tetrahedral lattice can be formed so that vertices of a cube not shared with the inscribed tetrahedron are shared with other tetrahedrons. Lattice points of such tetrahedral lattice correspond to the nodes of Group ② mentioned above. However, the tetrahedral lattice shown by dashed green line in the diagram has no common vertices with lattice shown by dashed brown line. That is, the cube side is shorter than the tetrahedron side, and two tetrahedral lattices are adjacent, but interactions do not propagate between nodes belonging to the different lattices.

As a solution to this problem, a method was proposed [6] to configure a cube by arranging rectangular triangular pyramids on every face of a regular tetrahedron as shown in Fig. A2. Here the pyramid sides not shared with the regular tetrahedron coincide with the cube sides; therefore,

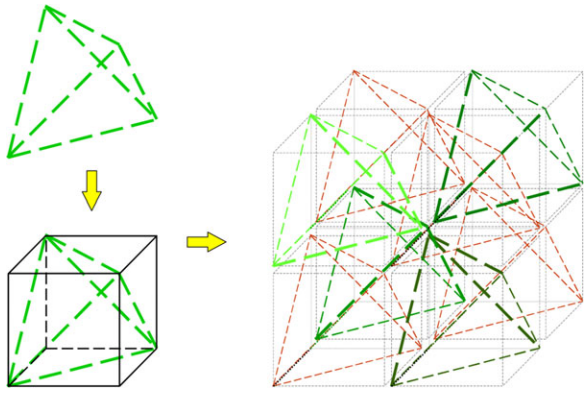

Fig. A1. Continuous arrangement of regular tetrahedrons inscribed in cubic structure. [Color figure can be viewed at wileyonlinelibrary.com]

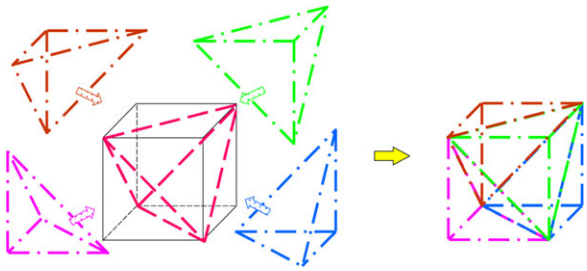

Fig. A2. Cubic structure constructed from regular tetrahedron and four right angle triangular pyramids. [Color figure can be viewed at wileyonlinelibrary.com]

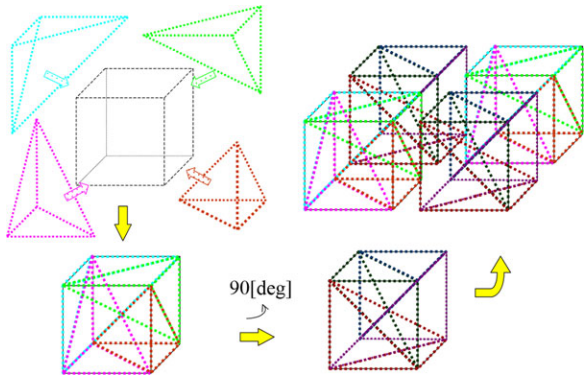

Fig. A3. Continuous arrangement of cubic structure that includes four tetrahedrons and consists of three kinds of diagonal lines. [Color figure can be viewed at wileyonlinelibrary.com]

lattice points obtained through continuous arrangement of such cubes correspond to the nodes of Groups ① and ② mentioned above.

A method was also proposed [6] to consider interactions between nodes placed at space diagonals of cubes. In this case, regular tetrahedrons are not regarded, four trigonal pyramids configured of cube's sides, face diagonals, and space diagonals are arranged so as to consider interactions between nodes placed at every vertex of the cube. An example of such arrangement is shown in Fig. A3. Lattice points obtained through continuous arrangement of such cubes correspond to the nodes of Groups ①, ②, and ③ mentioned above. Connections between all nodes can be considered if such cubes are continuously arranged while rotated.

Our analysis of shortages of the above methods resulted in adoption of the representation proposed in this study.

AUTHORS (from left to right)

Satoru Honma, member Born March 26, 1969. In 1993 Satoru HONMA graduated from Nihon University (College of Science and Technology), and in 1997 he graduated from Tokyo Medical and Dental University (Faculty of Medicine). In 2002 he completed doctorate at the University (Graduate School of Heath Care Sciences), and in 2003 he was employed by the University as assistant, and since 2004 he has been employed as assistant professor at Graduate School of Heath Care Sciences. He is a Doctor of Health Care Sciences.

Hidetoshi Wakamatsu, nonmember Born November 15, 1946. In 1972 Hidetoshi WAKAMATSU completed postgraduate studies at Yokohama National University, and he was employed as assistant by Tokyo Medical and Dental University, then he was employed as assistant professor at Ashikaga Institute of Technology, and as professor at University of Fukui. He is now professor emeritus at Tokyo Medical and Dental University. From 1973 to 1975 he was a visiting researcher at University of Erlangen-Nuremberg due to German Academic Exchange Service (DAAD). He is also a visiting professor at Oregon State University. He is a Doctor of Engineering.